Exclusive decays $J/\psi \to D_{(s)}^{(*)-}\ell^+\nu_\ell$ in a covariant constituent quark model with infrared confinement

M. A. Ivanov[1,*] and C. T. Tran[1,2,3,†]

[1]*Bogoliubov Laboratory of Theoretical Physics, Joint Institute for Nuclear Research, 141980 Dubna, Russia*

[2]*Advanced Center for Physics, Institute of Physics, Vietnam Academy of Science and Technology, Hanoi 100000, Vietnam*

[3]*Department of General and Applied Physics, Moscow Institute of Physics and Technology, 141700 Dolgoprudny, Russia*

We investigate the exclusive semileptonic decays $J/\psi \to D_{(s)}^{(*)-}\ell^+\nu_\ell$, where $\ell = e, \mu$, within the Standard Model. The relevant transition form factors are calculated in the framework of a relativistic constituent quark model with built-in infrared confinement. Our calculations predict the branching fractions $\mathcal{B}(J/\psi \to D_{(s)}^{(*)-}\ell^+\nu_\ell)$ to be of the order of 10^{-10} for $D_s^{(*)-}$ and 10^{-11} for $D^{(*)-}$. Most of our numerical results are consistent with other theoretical studies. However, some branching fractions are larger than those calculated in QCD sum rules approaches but smaller than those obtained in the covariant light-front quark model by a factor of about 2–3.

I. INTRODUCTION

Low lying states of quarkonia systems similar to J/ψ usually decay through intermediate photons or gluons produced by the parent $q\bar{q}$ quark pair annihilation [1]. As a result, strong and electromagnetic decays of J/ψ have been largely investigated while weak decays of J/ψ have been put aside for decades. However, in the last few years many improvements in instruments and experimental techniques, in particular, the luminosity of colliders, have led to observation of many rare processes including the extremely rare decays $B_{(s)}^0 \to \mu^+\mu^-$, announced lately by the CMS and LHCb collaborations [2]. The branching fractions were measured to be $\mathcal{B}(B_s^0 \to \mu^+\mu^-) = (2.8_{-0.6}^{+0.7}) \times 10^{-9}$ and $\mathcal{B}(B^0 \to \mu^+\mu^-) = (3.9_{-1.4}^{+1.6}) \times 10^{-10}$. This raises the hope that one may also explore the rare weak decays of charmonium and draws researchers' attention back to these modes.

Recently, BESIII Collaboration reported on their search for semileptonic weak decays $J/\psi \to D_s^{(*)-}e^+\nu_e + $ c.c. [3], where "+c.c." indicates that the signals were sum of these modes and the relevant charge conjugated ones. The results at 90% confidence level were found to be $\mathcal{B}(J/\psi \to D_s^-e^+\nu_e + $ c.c.$) < 1.3 \times 10^{-6}$ and $\mathcal{B}(J/\psi \to D_s^{*-}e^+\nu_e + $ c.c.$) < 1.8 \times 10^{-6}$. Although these upper limits are far above the predicted values within the Standard Model (SM), which are of the order of 10^{-8}–10^{-10} [4–6], one should note that this was the first time an experimental constraint on the branching fraction $\mathcal{B}(J/\psi \to D_s^{*-}e^+\nu_e + $ c.c.$)$ was set, and moreover, the constraint on the branching

fraction $\mathcal{B}(J/\psi \to D_s^-e^+\nu_e + $ c.c.$)$ was 30 times more stringent than the previous one [7]. With a huge data sample of 10^{10} J/ψ events accumulated each year, BESIII is expected to detect these decays, even at SM levels, in the near future.

From the theoretical point of view, these weak decays are of great importance since they may lead to better understanding of nonperturbative QCD effects taking place in transitions of heavy quarkonia. Moreover, the semileptonic modes $J/\psi \to D_{(s)}^{(*)}\ell\nu$, as three-body weak decays of a vector meson, supply plentiful information about the polarization observables that can be used to probe the hidden structure and dynamics of hadrons. Additionally, these decays may also provide some hints of new physics beyond the SM, such as TopColor models [8], the minimal supersymmetric Standard Model (MSSM) with or without R-parity [9], and the two-Higgs-doublet models (2HDMs) [10,11].

The very first estimate of $\mathcal{B}(J/\psi \to D_s^{(*)}\ell\nu)$ was made based on the (approximate) spin symmetry of heavy mesons, giving an inclusive branching fraction of $(0.4$–$1.0) \times 10^{-8}$, summed over D_s, D_s^*, e, μ and both charge conjugate modes [4]. In this work the transition form factors were parametrized through a universal function, similar to the Isgur-Wise function in the heavy quark limit. However, the zero-recoil approximation adopted in calculating the hadronic matrix elements led to large uncertainties in the decay width evaluation. For that reason, the author of [4] noted that these results should be viewed as an estimate suggesting experimental searching, rather than a definite prediction. Recently, by employing QCD sum rules (QCD SR) [5] or making use of the covariant light-front quark model (LFQM) [6], new theoretical

*[*]ivanovm@theor.jinr.ru
[†]ctt@theor.jinr.ru, tranchienthang1347@gmail.com

studies found the branching fractions of $J/\psi \to D_s^{(*)-}e^+\nu_e + \text{c.c.}$ to be of the order of 10^{-10}. However, the results presented in [6] were about 2–8 times larger than those calculated in [5]. Besides, one can significantly reduce hadronic uncertainties and other physical constants like G_F and $|V_{cs}|$ by considering the ratio of branching fractions $R \equiv \mathcal{B}(J/\psi \to D_s^*\ell\nu)/\mathcal{B}(J/\psi \to D_s\ell\nu)$. This ratio had been predicted to be $\simeq 1.5$ in [4] while the recent study [5] suggested $R \simeq 3.1$. Clearly, more theoretical studies and cross-check are necessary.

In the present work we offer an alternative approach to the investigation of the exclusive decays $J/\psi \to D_{(s)}^{(*)-}\ell^+\nu_\ell$, in which we employ the covariant constituent quark model with built-in infrared confinement [for short, confined covariant quark model (CCQM)] as dynamical input to calculate the nonperturbative transition matrix elements. Our paper is organized as follows: In Sec. II, we set up our framework by briefly introducing the CCQM. Section III contains the definitions and derivations of the form factors of the decays $J/\psi \to D_{(s)}^{(*)-}\ell^+\nu_\ell$ based on the effective Hamiltonian formalism. In this section we also describe in some detail how calculation of the form factors proceeds in our approach. Section IV is devoted to the numerical results for the form factors, including comparison with the available data. Section V contains our numerical results for the branching fractions. And finally, we make a brief summary of our main results in Sec. VI.

II. MODEL

The CCQM has been developed in some of our earlier papers (see [12] and references therein). In the CCQM framework one starts with an effective Lagrangian describing the coupling of a meson H to its constituent quarks q_1 and q_2,

$$
\mathcal{L}_{\text{int}}(x) = g_H H(x) \int dx_1
$$
$$
\times \int dx_2 F_H(x; x_1, x_2)[\bar{q}_2(x_2)\Gamma_H q_1(x_1)] + \text{H.c.},
\tag{1}
$$

where Γ_H is the relevant Dirac matrix and g_H is the coupling constant. The vertex function F_H is related to the scalar part of the Bethe-Salpeter amplitude and characterizes the finite size of the meson. Transitions between mesons are evaluated by one-loop Feynman diagrams with free quark propagators. The high energy divergence of quark loops is tempered by nonlocal Gaussian-type vertex functions with a falloff behavior. We adopt the following form,

$$
F_H(x; x_1, x_2) = \delta(x - w_1 x_1 - w_2 x_2)\Phi_H((x_1 - x_2)^2),
\tag{2}
$$

where $w_i = m_{q_i}/(m_{q_1} + m_{q_2})$. This form of F_H is invariant under the translation $F_H(x + a; x_1 + a, x_2 + a) = F_H(x; x_1, x_2)$, which is necessary for the Lorentz invariance of the Lagrangian (1).

We adopt a Gaussian form for the vertex function:

$$
\tilde{\Phi}_H(-p^2) = \int dx e^{ipx}\Phi_H(x^2) = e^{p^2/\Lambda_H^2}.
\tag{3}
$$

The parameter Λ_H characterizes the size of the meson. The calculations of the Feynman diagrams proceed in the Euclidean region where $p^2 = -p_E^2$ and therefore the vertex function has the appropriate falloff behavior to provide for the ultraviolet convergence of the loop integral.

The normalization of particle-quark vertices is provided by the compositeness condition [13]

$$
Z_H = 1 - \Pi_H'(m_H^2) = 0,
\tag{4}
$$

where Z_H is the wave function renormalization constant of the meson H and Π_H' is the derivative of the meson mass function. To better understand the physical meaning of the compositeness condition we want to remind the reader that the constant $Z_H^{1/2}$ can be viewed as the matrix element between the physical particle state and the corresponding bare state. The compositeness condition $Z_H = 0$ implies that the physical bound state does not contain the bare state. The constituents are virtual and they are introduced to realize the interaction described by the Lagrangian (1). As a result of the interaction, the physical particle becomes dressed and its mass and wave function are renormalized. Technically, the compositeness condition allows one to evaluate the coupling constant g_H. The meson mass function in (4) is defined by the Feynman diagram shown in Fig. 1. It has the explicit form

$$
\Pi_P(p) = 3g_P^2 \int \frac{dk}{(2\pi)^4 i} \tilde{\Phi}_P^2(-k^2)
$$
$$
\times \text{tr}[S_1(k + w_1 p)\gamma^5 S_2(k - w_2 p)\gamma^5],
\tag{5}
$$

and

$$
\Pi_V(p) = g_V^2 \left[g^{\mu\nu} - \frac{p^\mu p^\nu}{p^2}\right] \int \frac{dk}{(2\pi)^4 i} \tilde{\Phi}_V^2(-k^2)
$$
$$
\times \text{tr}[S_1(k + w_1 p)\gamma_\mu S_2(k - w_2 p)\gamma_\nu],
\tag{6}
$$

for a pseudoscalar meson and a vector meson, respectively. Note that we use the free quark propagator
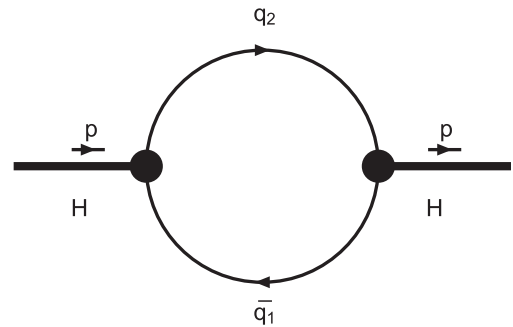

FIG. 1. One-loop self-energy diagram for a meson.

$$S_i(k) = \frac{1}{m_{q_i} - k - i\epsilon}, \qquad (7)$$

where m_{q_i} is the constituent quark mass.

The confinement of quarks is embedded in an effective way: first, by introducing a scale integration in the space of α-parameters; and second, by truncating this scale integration on the upper limit that corresponds to an infrared cutoff. By doing this one removes all possible thresholds in the quark diagram. The cutoff parameter is taken to be universal. Other model parameters are adjusted by fitting to available experimental data. Once these parameters are fixed, one can employ the CCQM as a frame-independent tool for hadronic calculation. One of the advantages of the CCQM is that in this framework the full physical range of momentum transfer is available, making calculation of hadronic quantities straightforward without any extrapolation.

III. HADRONIC MATRIX ELEMENTS

The effective Hamiltonian describing the semileptonic decays $J/\psi \to D^{(*)-}_{(s)} \ell^+ \nu_\ell$ is given by

$$\mathcal{H}_{\text{eff}}(c \to q\ell^+\nu_\ell) = \frac{G_F}{\sqrt{2}} V_{cq}[\bar{q}O_\mu c][\bar{\nu}_\ell O^\mu \ell], \qquad (8)$$

where $q = s, d$, and $O^\mu = \gamma^\mu(1 - \gamma_5)$ is the weak Dirac matrix with left chirality.

In the CCQM the hadronic matrix elements of the semileptonic J/ψ meson decays are defined by the diagram in Fig. 2 and are given by

$$\langle D^-_{(s)}(p_2)|\bar{q}O_\mu c|J/\psi(\epsilon_1, p_1)\rangle$$
$$= \epsilon_1^\alpha T^{\text{VP}}_{\mu\alpha}$$
$$T^{\text{VP}}_{\mu\alpha} = 3g_{J/\psi}g_P \int \frac{d^4k}{(2\pi)^4 i} \tilde{\Phi}_{J/\psi}[-(k + w_{13}p_1)^2]$$
$$\times \tilde{\Phi}_P[-(k + w_{23}p_2)^2]$$
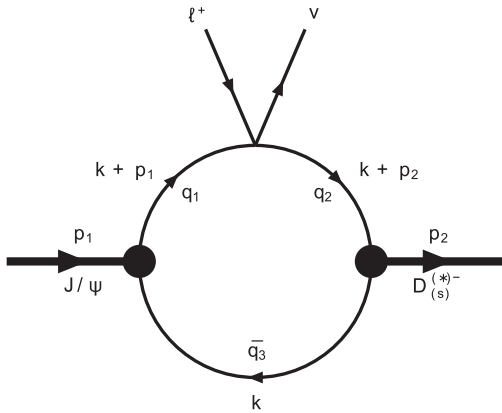$$\times \text{tr}[S_2(k + p_2)O_\mu S_1(k + p_1)\gamma_\alpha S_3(k)\gamma_5], \qquad (9)$$

FIG. 2. Diagram for J/ψ meson semileptonic decays.

$$\langle D^{*-}_{(s)}(\epsilon_2, p_2)|\bar{q}O_\mu c|J/\psi(\epsilon_1, p_1)\rangle$$
$$= \epsilon_1^\alpha \epsilon_2^{*\beta} T^{\text{VV}}_{\mu\alpha\beta}$$
$$T^{\text{VV}}_{\mu\alpha\beta} = 3g_{J/\psi}g_V \int \frac{d^4k}{(2\pi)^4 i} \tilde{\Phi}_{J/\psi}[-(k + w_{13}p_1)^2]$$
$$\times \tilde{\Phi}_V[-(k + w_{23}p_2)^2]$$
$$\times \text{tr}[S_2(k + p_2)O_\mu S_1(k + p_1)\gamma_\alpha S_3(k)\gamma_\beta]. \qquad (10)$$

We use the on-shell conditions $\epsilon_1 \cdot p_1 = 0$, $\epsilon_2^* \cdot p_2 = 0$, and $p_i^2 = m_i^2$. Because there are three quark types involved in the transition, we have introduced a two-subscript notation $w_{ij} = m_{q_j}/(m_{q_i} + m_{q_j})$ $(i, j = 1, 2, 3)$ such that $w_{ij} + w_{ji} = 1$.

The loop integrations in Eqs. (9) and (10) are done with the help of the Fock-Schwinger representation of the quark propagator

$$S_q(k + p) = \frac{1}{m_q - k - p} = \frac{m_q + k + p}{m_q^2 - (k + p)^2}$$
$$= (m_q + k + p) \int_0^\infty d\alpha e^{-\alpha[m_q^2 - (k+p)^2]}, \qquad (11)$$

where k is the loop momentum and p is the external momentum. As described later on, the use of the Fock-Schwinger representation allows one to do tensor loop integrals in a very efficient way since one can convert loop momenta into derivatives of the exponent function.

All loop integrations are performed in Euclidean space. The transition from Minkowski space to Euclidean space is performed by using the Wick rotation

$$k_0 = e^{i\frac{\pi}{2}}k_4 = ik_4 \qquad (12)$$

so that $k^2 = k_0^2 - \vec{k}^2 = -k_4^2 - \vec{k}^2 = -k_E^2 \leq 0$. Simultaneously one has to rotate all external momenta, i.e. $p_0 \to ip_4$ so that $p^2 = -p_E^2 \leq 0$. Then the quadratic form in Eq. (11) becomes positive definite,

$$m_q^2 - (k + p)^2 = m_q^2 + (k_E + p_E)^2 > 0,$$

and the integral over α is absolutely convergent. We will keep the Minkowski notation to avoid excessive relabeling. We simply imply that $k^2 \leq 0$ and $p^2 \leq 0$.

Collecting the representations for the vertex functions and quark propagators given by Eqs. (3) and (11), respectively, one can perform the Gaussian integration in the expressions for the matrix elements in Eqs. (9) and (10). The exponent has the form $ak^2 + 2kr + z_0$, where $r = bp$. Using the following properties,

$$k^\mu \exp(ak^2 + 2kr + z_0) = \tfrac{1}{2}\tfrac{\partial}{\partial r_\mu}\exp(ak^2 + 2kr + z_0)$$

$$k^\mu k^\nu \exp(ak^2 + 2kr + z_0) = \tfrac{1}{2}\tfrac{\partial}{\partial r_\mu}\tfrac{1}{2}\tfrac{\partial}{\partial r_\nu}\exp(ak^2 + 2kr + z_0)$$

$$\text{etc.}$$

$$(13)$$

one can replace k by $\partial_r = \gamma^\mu \frac{\partial}{\partial r_\mu}$ which allows one to exchange the tensor integrations for a differentiation of the Gaussian exponent $e^{-r^2/a}$ which appears after integration over loop momentum. The r-dependent Gaussian exponent $e^{-r^2/a}$ can be moved to the left through the differential operator ∂_r by using the following properties,

$$\frac{\partial}{\partial r_\mu} e^{-r^2/a} = e^{-r^2/a}\left[-\frac{2r^\mu}{a} + \frac{\partial}{\partial r_\mu}\right],$$

$$\frac{\partial}{\partial r_\mu}\frac{\partial}{\partial r_\nu} e^{-r^2/a} = e^{-r^2/a}\left[-\frac{2r^\mu}{a} + \frac{\partial}{\partial r_\mu}\right]\cdot\left[-\frac{2r^\nu}{a} + \frac{\partial}{\partial r_\nu}\right],$$

$$\text{etc.} \qquad (14)$$

Finally, one has to move the derivatives to the right by using the commutation relation

$$\left[\frac{\partial}{\partial r_\mu}, r^\nu\right] = g^{\mu\nu}. \qquad (15)$$

The last step has been done by using a FORM code which works for any numbers of loops and propagators. In the remaining integrals over the Fock-Schwinger parameters $0 \le \alpha_i < \infty$ we introduce an additional integration which converts the set of Fock-Schwinger parameters into a simplex. We use the transformation

$$\prod_{i=1}^{n}\int_0^\infty d\alpha_i f(\alpha_1, \ldots, \alpha_n)$$

$$= \int_0^\infty dt\, t^{n-1}\prod_{i=1}^{n}\int d\alpha_i \delta\left(1 - \sum_{i=1}^{n}\alpha_i\right) f(t\alpha_1, \ldots, t\alpha_n).$$

$$(16)$$

The integral over t is well defined and convergent below the threshold $p_1^2 < (m_{q_c} + m_q)^2$. The convergence of the integral above threshold $p_1^2 \ge (m_c + m_q)^2$ is guaranteed by the addition of a small imaginary to the quark mass, i.e. $m_q \to m_q - i\epsilon, \epsilon > 0$ in the quark propagator. It allows one to rotate the integration variable t to the imaginary axis $t \to it$. As a result the integral becomes convergent but obtains an imaginary part corresponding to quark pair production.

However, by cutting the scale integration at the upper limit corresponding to the introduction of an infrared cutoff

$$\int_0^\infty dt(\ldots) \to \int_0^{1/\lambda^2} dt(\ldots), \qquad (17)$$

one can remove all possible thresholds present in the initial quark diagram [14]. Thus the infrared cutoff parameter λ effectively guarantees the confinement of quarks within hadrons. This method is quite general and can be used for diagrams with an arbitrary number of loops and propagators. In the CCQM the infrared cutoff parameter λ is taken to be universal for all physical processes [15].

Finally, the matrix elements in Eqs. (9) and (10) are written down as linear combinations of the Lorentz structures multiplied by the scalar functions—form factors which depend on the momentum transfer squared. For the $V \to P$ transition one has

$$\langle D_{(s)}^-(p_2)|\bar{q}O_\mu c|J/\psi(\epsilon_1, p_1)\rangle$$

$$= \frac{\epsilon_1^\nu}{m_1 + m_2}[-g_{\mu\nu}pqA_0(q^2)$$

$$+ p_\mu p_\nu A_+(q^2) + q_\mu p_\nu A_-(q^2) + i\varepsilon_{\mu\nu\alpha\beta}p^\alpha q^\beta V(q^2)],$$

$$(18)$$

where $q = p_1 - p_2$, $p = p_1 + p_2$, $m_1 \equiv m_{J/\psi}$, $m_2 \equiv m_{D_{(s)}}$.

For comparison of results we relate our form factors to those defined, e.g., in [16], which are denoted by a superscript c. The relations read

$$A_+ = A_2^c,$$

$$A_0 = \frac{m_1 + m_2}{m_1 - m_2}A_1^c,$$

$$V = V^c,$$

$$A_- = \frac{2m_2(m_1 + m_2)}{q^2}(A_3^c - A_0^c). \qquad (19)$$

We note in addition that the form factors $A_i^c(q^2)$ satisfy the constraints

$$A_0^c(0) = A_3^c(0) \quad \text{and}$$

$$2m_2A_3^c(q^2) = (m_1 + m_2)A_1^c(q^2) - (m_1 - m_2)A_2^c(q^2)$$

$$(20)$$

to avoid the singularity at $q^2 = 0$.

In the case of the $V \to V$ transition we follow the authors in [5] and define the form factors as follows:

$$\langle D^{*-}_{(s)}(\epsilon_2, p_2)|\bar{q}O_\mu c|J/\psi(\epsilon_1, p_1)\rangle = \varepsilon_{\mu\nu\alpha\beta}\epsilon_1^\alpha\epsilon_2^{*\beta}\left[\left(p^\nu - \frac{m_1^2 - m_2^2}{q^2}q^\nu\right)A_1(q^2) + \frac{m_1^2 - m_2^2}{q^2}q^\nu A_2(q^2)\right]$$

$$+ \frac{i}{m_1^2 - m_2^2}\varepsilon_{\mu\nu\alpha\beta}p_1^\alpha p_2^\beta[A_3(q^2)\epsilon_1^\nu\epsilon_2^* \cdot q - A_4(q^2)\epsilon_2^{*\nu}\epsilon_1 \cdot q]$$

$$+ (\epsilon_1 \cdot \epsilon_2^*)[-p_\mu V_1(q^2) + q_\mu V_2(q^2)]$$

$$+ \frac{(\epsilon_1 \cdot q)(\epsilon_2^* \cdot q)}{m_1^2 - m_2^2}\left[\left(p_\mu - \frac{m_1^2 - m_2^2}{q^2}q_\mu\right)V_3(q^2) + \frac{m_1^2 - m_2^2}{q^2}q_\mu V_4(q^2)\right]$$

$$- (\epsilon_1 \cdot q)\epsilon^*_{2\mu}V_5(q^2) + (\epsilon_2^* \cdot q)\epsilon_{1\mu}V_6(q^2). \tag{21}$$

The form factors in our model are represented by the threefold integrals which are calculated by using FORTRAN codes in the full kinematical momentum transfer region.

IV. FORM FACTORS

Before listing our numerical results we need to specify parameters of the CCQM that cannot be evaluated from first principles. They are the size parameter of hadrons Λ, the universal infrared cutoff parameter λ and the constituent quark masses m_{q_i}. These parameters are determined by a least-squares fit of calculated meson leptonic decay constants and several fundamental electromagnetic decays to experimental data and/or lattice simulations within a root-mean-square deviation of 15% [17]. This value can provide a reasonable estimate of our theoretical error since the calculations in our work are, in principle, not different from those used in the fit. For example, based on a widespread application in a previous paper [18], we suggested that a reasonable estimate of our theoretical error is 15%.

The most recent fit results for those parameters involved in this paper are given in (22) (all in GeV):

$m_{u/d}$	m_s	m_c	λ	$\Lambda_{J/\psi}$	Λ_{D^*}	$\Lambda_{D_s^*}$	Λ_D	Λ_{D_s}
0.241	0.428	1.67	0.181	1.74	1.53	1.56	1.60	1.75.

$$\tag{22}$$

Model-independent parameters and other physical constants like Cabibbo-Kobayashi-Maskawa matrix elements, mass and decay width of particles are taken from [7]. For clarity we note that we use the values $|V_{cd}| = 0.225$ and $|V_{cs}| = 0.986$.

We present our results for leptonic decay constants of J/ψ and $D^{(*)}_{(s)}$ mesons in Table I. We also list the values of these constants obtained from experiments or other theoretical studies for comparison. One can see that our calculated values are consistent (within 10%) with results of other studies.

In Figs. 3–5 we present the q^2 dependence of calculated form factors of the $J/\psi \to D^{(*)}_{(s)}$ transitions in the full range of momentum transfer $0 \le q^2 \le q^2_{\max} = (m_{J/\psi} - m_{D^{(*)}_{(s)}})^2$.

We found that the form factors A_3 and A_4 defined in (21) are very similar to each other. As mentioned earlier, the CCQM allows one to evaluate form factors in the full kinematical range including the near-zero recoil region. This feature is one of those that distinguish the CCQM from other frameworks like QCD SR and some other approaches. For example, the physical region of q^2 for $J/\psi \to D^-\ell^+\nu_\ell$ is $0 \le q^2 \le (m_{J/\psi} - m_{D^-})^2 \simeq 1.51 \text{ GeV}^2$. However, within the QCD SR approach, the authors of [5] had to restrict their calculations in the range of $q^2 \in [0, 0.47] \text{ GeV}^2$ to avoid additional singularities and then use an extrapolation to obtain the form factors in large q^2 region. As a result, the extrapolation type becomes more sensitive.

The results of our numerical calculation are well represented by a double-pole parametrization

$$F(q^2) = \frac{F(0)}{1 - as + bs^2},$$
$$s = \frac{q^2}{m_1^2}, \tag{23}$$

where $m_1 = m_{J/\psi}$. The double-pole approximation is quite accurate. The relative error relative to the exact results is less than 1% over the entire q^2 range, as demonstrated in Fig. 6.

TABLE I. Results for the leptonic decay constants f_H in MeV.

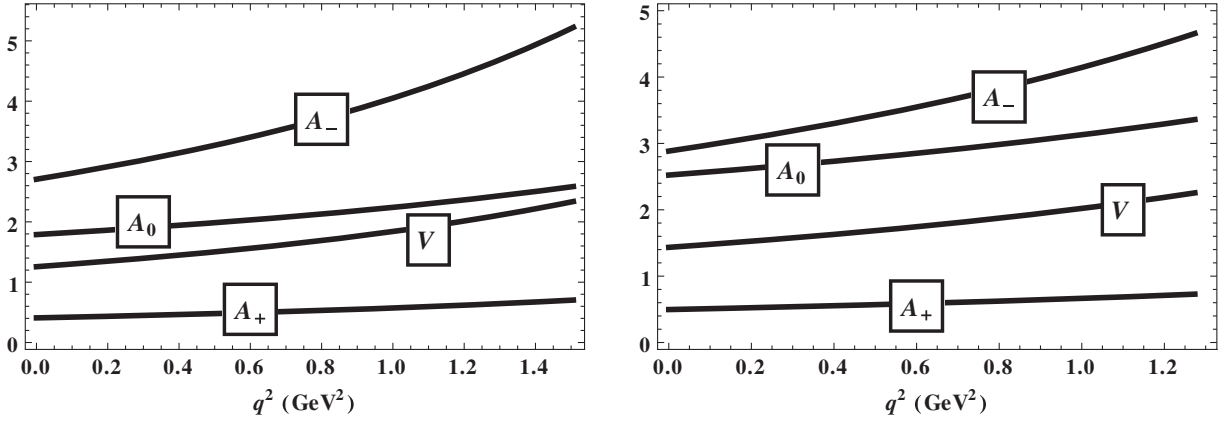|	This work	Other	Reference
$f_{J/\psi}$	415.0	418 ± 9	LAT and QCD SR [19]
f_D	206.1	204.6 ± 5.0	PDG [7]
f_{D^*}	244.3	$245(20)^{+3}_{-2}$	LAT [20]
		$278 \pm 13 \pm 10$	LAT [21]
		$252.2 \pm 22.3 \pm 4$	QCD SR [22]
f_{D_s}	257.5	257.5 ± 4.6	PDG [7]
$f_{D_s^*}$	272.0	$272(16)^{+3}_{-20}$	LAT [20]
		311 ± 9	LAT [21]
		$305.5 \pm 26.8 \pm 5$	QCD SR [22]
f_{D_s}/f_D	1.249	1.258 ± 0.038	PDG [7]
$f_{D_s^*}/f_{D^*}$	1.113	$1.16 \pm 0.02 \pm 0.06$	LAT [21]

FIG. 3.   Our results for the form factors of the $J/\psi \to D$ (left) and $J/\psi \to D_s$ (right) transitions.

FIG. 4.   Our results for the form factors of the $J/\psi \to D^*$ transitions. One has to note that in the left panel $A_1(0) = A_2(0)$ and $A_3(q^2) \equiv A_4(q^2)$.
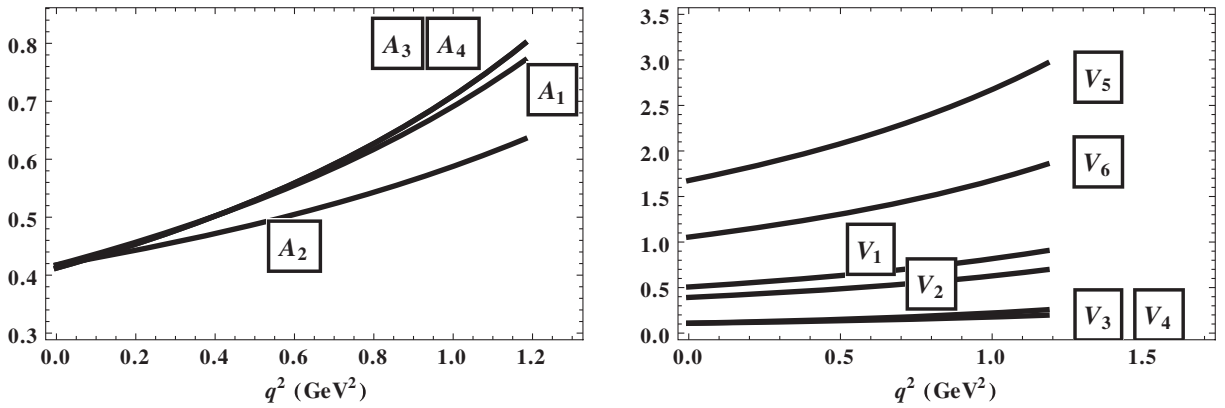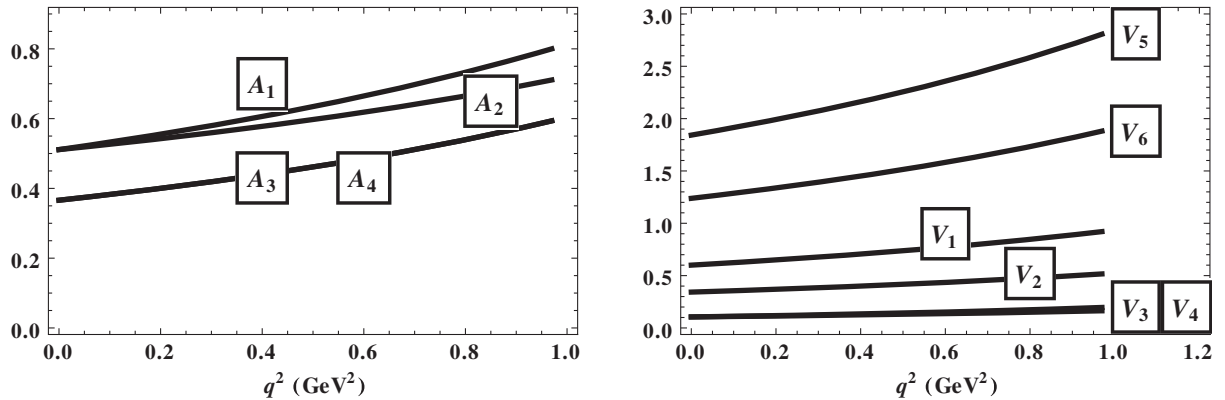

FIG. 5.   Our results for the form factors of the $J/\psi \to D_s^*$ transitions. One has to note that in the left panel $A_1(0) = A_2(0)$ and $A_3(q^2) \equiv A_4(q^2)$.

For the $J/\psi \to D_{(s)}^{(*)}$ transitions the parameters of the dipole approximation are displayed in Tables II and III.

In Tables IV and V we compare the values of our form factors at $q^2 = 0$ (maximum recoil) with those obtained within QCD SR [5] and LFQM [6]. Our results are more consistent with those in [5]. For example, our predictions for the form factors at $q^2 = 0$ differ from the results of [5] within 40% while the discrepancy can come to a factor of 4 compared with the results of [6].
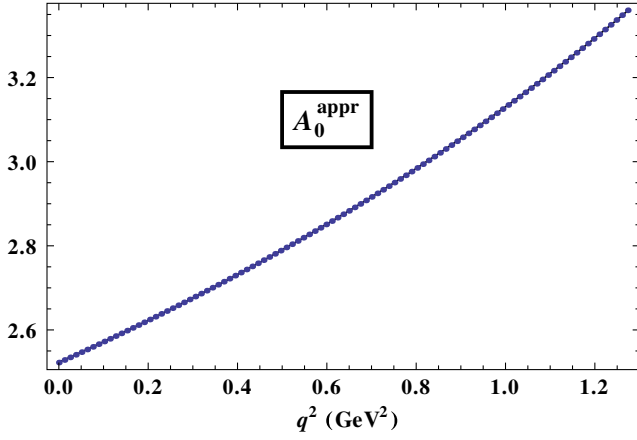
FIG. 6 (color online). Comparison of the $A_0(q^2)$ form factor for the $J/\psi \to D_s$ transition calculated by FORTRAN code (dotted) with parametrization given by Eq. (23) (solid).

TABLE II. Parameters of the dipole approximation for $J/\psi \to D_{(s)}$ form factors.

	$J/\psi \to D$				$J/\psi \to D_s$			
	A_0	A_+	A_-	V	A_0	A_+	A_-	V
F(0)	1.79	0.41	2.71	1.26	2.52	0.50	2.88	1.43
a	1.87	2.90	3.41	3.24	1.81	2.53	3.10	2.94
b	−0.56	1.43	2.21	1.89	−0.47	0.98	1.76	1.48

where the upper/lower sign refers to the two $(\ell^-\bar{\nu}_\ell)/$ $(\ell^+\nu_\ell)$ configurations. The sign change can be seen to result from the parity violating part of the lepton tensors. In our case we have to use the lower sign in Eq. (25). Summing up the vector polarizations, one finds the decay rate

$$\Gamma(J/\psi \to D_{(s)}^{(*)-}\ell^+\nu_\ell) = \frac{G_F^2}{(2\pi)^3} \frac{|V_{cq}|^2}{64m_1^3} \int_{m_\ell^2}^{(m_1-m_2)^2} dq^2$$

$$\times \int_{s_1^-}^{s_1^+} ds_1 \frac{1}{3} H_{\mu\nu} L^{\mu\nu}. \qquad (26)$$

Here $m_1 = m_{J/\psi}$, $m_2 = m_D$ and $s_1 = (p_D + p_\ell)^2$. The upper and lower bounds of s_1 are given by

$$s_1^\pm = m_2^2 + m_\ell^2 - \frac{1}{2q^2}[(q^2 - m_1^2 + m_2^2)(q^2 + m_\ell^2)$$

$$\mp \lambda^{1/2}(q^2, m_1^2, m_2^2)\lambda^{1/2}(q^2, m_\ell^2, 0)], \qquad (27)$$

where $\lambda(x, y, z) \equiv x^2 + y^2 + z^2 - 2(xy + yz + zx)$ is the Källén function.

The hadron tensor reads

V. NUMERICAL RESULTS

The invariant matrix element for the decay $J/\psi \to D_{(s)}^{(*)-}\ell^+\nu_\ell$ is written down as

$$\mathcal{M} = \frac{G_F}{\sqrt{2}} V_{cq} \langle D^- | \bar{q} O_\mu c | J/\psi \rangle [\bar{\nu}_\ell O^\mu \ell]. \qquad (24)$$

The unpolarized lepton tensor for the process $W_{\text{off-shell}}^- \to \ell^-\bar{\nu}_\ell$ ($W_{\text{off-shell}}^+ \to \ell^+\nu_\ell$) is given by [23]

$$L^{\mu\nu} = \begin{cases} \text{tr}[(\not{p}_\ell + m_\ell)O^\mu \not{p}_{\nu_\ell} O^\nu] & \text{for } W_{\text{off-shell}}^- \to \ell^-\bar{\nu}_\ell \\ \text{tr}[(\not{p}_\ell - m_\ell)O^\nu \not{p}_{\nu_\ell} O^\mu] & \text{for } W_{\text{off-shell}}^+ \to \ell^+\nu_\ell \end{cases}$$

$$= 8(p_\ell^\mu p_{\nu_\ell}^\nu + p_\ell^\nu p_{\nu_\ell}^\mu - p_\ell \cdot p_{\nu_\ell} g^{\mu\nu} \pm i\varepsilon^{\mu\nu\alpha\beta} p_{\ell\alpha} p_{\nu_\ell\beta})$$

$$\qquad (25)$$

$$H_{\mu\nu} = \begin{cases} T_{\mu\alpha}^{VP}\left(-g^{\alpha\alpha'} + \frac{p_1^\alpha p_1^{\alpha'}}{m_1^2}\right) T_{\nu\alpha'}^{VP\dagger} & \text{for } V \to P \text{ transition} \\ T_{\mu\alpha\beta}^{VV}\left(-g^{\alpha\alpha'} + \frac{p_1^\alpha p_1^{\alpha'}}{m_1^2}\right)\left(-g^{\beta\beta'} + \frac{p_2^\beta p_2^{\beta'}}{m_2^2}\right) T_{\nu\alpha'\beta'}^{VV\dagger} & \text{for } V \to V \text{ transition.} \end{cases} \qquad (28)$$

We present our results for the branching fractions in Table VI together with results of other theoretical studies based on QCD SR and LFQM for comparison. It is worth mentioning that all values for $\mathcal{B}(J/\psi \to D_{(s)}^*\ell\nu)$ are fully consistent with those in [5]. Regarding $\mathcal{B}(J/\psi \to D_{(s)}\ell\nu)$, our results are larger than those in [5] by a factor of 2–3. We think this discrepancy is mainly due to the values of the meson leptonic decay constants $f_D = 166$ MeV and $f_{D_s} = 189$ MeV used in [5], which are much smaller than $f_D = 206.1$ MeV and $f_{D_s} = 257.5$ MeV used in our present paper. In contrast, the constants $f_{D^*} = 240$ MeV and

$f_{D_s^*} = 262$ MeV used in [5] are very close to our values of $f_{D^*} = 244.3$ MeV and $f_{D_s^*} = 272.0$ MeV, resulting in a full agreement in $\mathcal{B}(J/\psi \to D_{(s)}^*\ell\nu)$ between the two studies. Comparing with another study, our results for $\mathcal{B}(J/\psi \to D_{(s)}\ell\nu)$ are smaller than those in [6] by a factor of 2–3.

It is interesting to consider the ratio $R \equiv \mathcal{B}(J/\psi \to D_s^*\ell\nu)/\mathcal{B}(J/\psi \to D_s\ell\nu)$, where a large part of the theoretical and experimental uncertainties cancels. We list in (29) all available predictions for R up till now:

TABLE III. Parameters of the dipole approximation for $J/\psi \to D^*_{(s)}$ form factors.

	A_1	A_2	A_3	A_4	V_1	V_2	V_3	V_4	V_5	V_6
					$J/\psi \to D^*$					
F(0)	0.42	0.42	0.41	0.41	0.51	0.39	0.11	0.11	1.68	1.05
a	4.20	2.75	4.46	4.46	3.98	3.85	4.03	6.00	3.88	3.85
b	3.87	−0.30	4.27	4.27	3.25	2.44	2.95	10.56	2.83	2.80
					$J/\psi \to D^*_s$					
F(0)	0.51	0.51	0.37	0.37	0.60	0.34	0.10	0.10	1.84	1.23
a	3.89	2.76	4.15	4.15	3.72	3.52	3.80	5.46	3.64	3.62
b	3.15	−0.18	3.57	3.57	2.72	1.94	2.53	8.82	2.39	2.37

TABLE IV. Comparison of $J/\psi \to D_{(s)}$ form factors at maximum recoil with those obtained in QCD SR and LFQM.

	$J/\psi \to D: q^2 = 0$				$J/\psi \to D_s: q^2 = 0$			
	A_0	A_+	A_-	V	A_0	A_+	A_-	V
QCD SR [5]	1.09	0.34	$\cdots$	0.81	1.71	0.35	$\cdots$	1.07
LFQM [6]	2.75	0.18	$\cdots$	1.6	3.05	0.13	$\cdots$	1.8
Our results	1.79	0.41	2.71	1.26	2.52	0.50	2.88	1.43

TABLE V. Comparison of $J/\psi \to D^*_{(s)}$ form factors at maximum recoil with those obtained in QCD SR [5].

	A_1	A_2	A_3	A_4	V_1	V_2	V_3	V_4	V_5	V_6
					$J/\psi \to D^*: q^2 = 0$					
[5]	0.40	0.44	0.86	0.91	0.41	0.63	0.22	0.26	1.37	0.87
Our results	0.42	0.42	0.41	0.41	0.51	0.39	0.11	0.11	1.68	1.05
					$J/\psi \to D^*_s: q^2 = 0$					
[5]	0.53	0.53	0.91	0.91	0.54	0.69	0.24	0.26	1.69	1.14
Our results	0.51	0.51	0.37	0.37	0.60	0.34	0.11	0.11	1.84	1.24

TABLE VI. Semileptonic decay branching fractions of the J/ψ meson.

Mode	Unit	This work	QCD SR [5]	LFQM [6]
$J/\psi \to D^- e^+ \nu_e$	10^{-12}	17.1	$7.3^{+4.3}_{-2.2}$	51–57
$J/\psi \to D^- \mu^+ \nu_\mu$	10^{-12}	16.6	$7.1^{+4.2}_{-2.2}$	47–55
$J/\psi \to D_s^- e^+ \nu_e$	10^{-10}	3.3	$1.8^{+0.7}_{-0.5}$	5.3–5.8
$J/\psi \to D_s^- \mu^+ \nu_\mu$	10^{-10}	3.2	$1.7^{+0.7}_{-0.5}$	5.5–5.7
$J/\psi \to D^{*-} e^+ \nu_e$	10^{-11}	3.0	$3.7^{+1.6}_{-1.1}$	$\cdots$
$J/\psi \to D^{*-} \mu^+ \nu_\mu$	10^{-11}	2.9	$3.6^{+1.6}_{-1.1}$	$\cdots$
$J/\psi \to D_s^{*-} e^+ \nu_e$	10^{-10}	5.0	$5.6^{+1.6}_{-1.6}$	$\cdots$
$J/\psi \to D_s^{*-} \mu^+ \nu_\mu$	10^{-10}	4.8	$5.4^{+1.6}_{-1.5}$	$\cdots$

$$R \equiv \frac{\mathcal{B}(J/\psi \to D^*_s \ell \nu)}{\mathcal{B}(J/\psi \to D_s \ell \nu)} = \begin{cases} 1.5 & \text{M.A. Sanchis-Lonzano [4]} \\ 3.1 & \text{Y.M. Wang [5]} \\ 1.5 & \text{This work} \end{cases}. \qquad (29)$$

Wang's result for R is about two times greater than our prediction because their branching fraction $\mathcal{B}(J/\psi \to D_s \ell \nu)$ is about two times smaller than ours (mainly due to the leptonic decay constants). Therefore, we propose that the value $R \simeq 1.5$ is a reliable prediction.

Moreover, we also consider the ratios

$$R_1 \equiv \frac{\mathcal{B}(J/\psi \to D_s \ell \nu)}{\mathcal{B}(J/\psi \to D \ell \nu)} \quad \text{and} \quad R_2 \equiv \frac{\mathcal{B}(J/\psi \to D_s^* \ell \nu)}{\mathcal{B}(J/\psi \to D^* \ell \nu)},$$

(30)

which should be equal to $\frac{|V_{cs}|^2}{|V_{cd}|^2} \simeq 18.4$ under the $SU(3)$ flavor symmetry limit. These ratios are $R_1 \simeq 24.7$ and $R_2 \simeq 15.1$ in [5]. In this work we have the following values, $R_1 \simeq 19.3$ and $R_2 \simeq 16.6$, which suggest a relatively small $SU(3)$ symmetry breaking effect.

VI. SUMMARY AND CONCLUSIONS

Let us summarize the main results of our paper. We have calculated the hadronic form factors relevant to the semileptonic decay $J/\psi \to D_{(s)}^{(*)-} \ell^+ \nu_\ell$ in the framework of the confined covariant quark model. By using the calculated form factors and Standard Model parameters we have evaluated the decay rates and branching fractions. We have compared our results with those obtained in other approaches.

ACKNOWLEDGMENTS

[1] K. K. Sharma and R. C. Verma, Rare decays of psi and upsilon, Int. J. Mod. Phys. A **14**, 937 (1999).

[2] V. Khachatryan *et al.* (CMS and LHCb Collaborations), Observation of the rare $B_s^0 \to \mu^+ \mu^-$ decay from the combined analysis of CMS and LHCb data, Nature (London) **522**, 68 (2015).

[3] M. Ablikim *et al.* (BESIII Collaboration), Search for the weak decays $J/\psi \to D_s^{(*)} e \nu_e + $ c.c., Phys. Rev. D **90**, 112014 (2014).

[4] M. A. Sanchis-Lozano, On the search for weak decays of heavy quarkonium in dedicated heavy quark factories, Z. Phys. C **62**, 271 (1994).

[5] Y. M. Wang, H. Zou, Z. T. Wei, X. Q. Li, and C. D. Lu, The transition form-factors for semi-leptonic weak decays of J/ψ in QCD sum rules, Eur. Phys. J. C **54**, 107 (2008).

[6] Y. L. Shen and Y. M. Wang, J/ψ weak decays in the covariant light-front quark model, Phys. Rev. D **78**, 074012 (2008).

[7] K. A. Olive *et al.* (Particle Data Group Collaboration), Review of particle physics, Chin. Phys. C **38**, 090001 (2014).

[8] C. T. Hill, Topcolor assisted technicolor, Phys. Lett. B **345**, 483 (1995).

[9] S. P. Martin, A supersymmetry primer, Adv. Ser. Dir. High Energy Phys. **21**, 1 (2010).

[10] W. S. Hou, Enhanced charged Higgs boson effects in $B^- \to \tau \bar{\nu}$, $\mu \bar{\nu}$ and $b \to \tau \bar{\nu} + X$, Phys. Rev. D **48**, 2342 (1993).

[11] S. Baek and Y. G. Kim, Constraints on the R-parity violating couplings from $B^\pm \to l^\pm v$ decays, Phys. Rev. D **60**, 077701 (1999).

[12] M. A. Ivanov, J. G. Körner, S. G. Kovalenko, P. Santorelli, and G. G. Saidullaeva, Form factors for semileptonic, non-leptonic and rare $B(B_s)$ meson decays, Phys. Rev. D **85**, 034004 (2012).

[13] A. Salam, Lagrangian theory of composite particles, Nuovo Cimento **25**, 224 (1962); S. Weinberg, Elementary particle theory of composite particles, Phys. Rev. **130**, 776 (1963);

K. Hayashi, M. Hirayama, T. Muta, N. Seto, and T. Shirafuji, Fortschr. Phys. **15**, 625 (1967).

[14] T. Branz, A. Faessler, T. Gutsche, M. A. Ivanov, J. G. Körner, and V. E. Lyubovitskij, Relativistic constituent quark model with infrared confinement, Phys. Rev. D **81**, 034010 (2010).

[15] M. A. Ivanov, J. G. Körner, and C. T. Tran, Exclusive decays $B \to \ell^- \bar{\nu}$ and $B \to D^{(*)} \ell^- \bar{\nu}$ in the covariant quark model, arXiv:1508.02678.

[16] A. Khodjamirian, T. Mannel, and N. Offen, Form-factors from light-cone sum rules with B-meson distribution amplitudes, Phys. Rev. D **75**, 054013 (2007).

[17] M. A. Ivanov, J. G. Körner, and P. Santorelli, The semileptonic decays of the B_c meson, Phys. Rev. D **63**, 074010 (2001).

[18] M. A. Ivanov, J. G. Körner, S. G. Kovalenko, and C. D. Roberts, B- to light-meson transition form-factors, Phys. Rev. D **76**, 034018 (2007).

[19] D. Becirevic, G. Duplancic, B. Klajn, B. Melic, and F. Sanfilippo, Lattice QCD and QCD sum rule determination of the decay constants of η_c, J/ψ and h_c states, Nucl. Phys. **B883**, 306 (2014).

[20] D. Becirevic, P. Boucaud, J. P. Leroy, V. Lubicz, G. Martinelli, F. Mescia, and F. Rapuano, Nonperturbatively improved heavy—light mesons: Masses and decay constants, Phys. Rev. D **60**, 074501 (1999).

[21] D. Becirevic, V. Lubicz, F. Sanfilippo, S. Simula, and C. Tarantino, D-meson decay constants and a check of factorization in non-leptonic B-decays, J. High Energy Phys. 02 (2012) 042.

[22] W. Lucha, D. Melikhov, and S. Simula, Decay constants of the charmed vector mesons D^* and D_s^* from QCD sum rules, Phys. Lett. B **735**, 12 (2014).

[23] T. Gutsche, M. A. Ivanov, J. G. Körner, V. E. Lyubovitskij, P. Santorelli, and N. Habyl, Semileptonic decay $\Lambda_b \to \Lambda_c + \tau^- + \bar{\nu}_\tau$ in the covariant confined quark model, Phys. Rev. D **91**, 074001 (2015); **91**, 119907 (2015).